Chapter 5

Direction specific spatial summation in motion sensitive area MST

János A. Perge, Kenneth H. Britten and Richard J. A. van Wezel

Abstract
Self-motion through a structured environment produces complex motion patterns on our retina, called optic flow. Visual processing of optic flow implies the existence of cortical mechanisms that sum local motion signals both over space and direction. We studied these summation mechanisms in medial superior temporal (MST) area of the macaque. This cortical area contains neurons with selectivity for optic flow components. We investigated whether summation depends on the relative difference in motion direction of two local motion inputs. We presented small, spatial Gabor functions moving simultaneously at nine different locations in the receptive field. At each Gabor location, we presented a pseudorandom sequence of brief motion impulses in any of four different directions independent from the other Gabor locations. This stimulus presentation allowed us to analyze a large number of Gabor combinations over both space and direction. We probed the mechanisms of summation by comparing the effect of Gabor pairs to the summed effect of their components. We found that summation is different if two local motion inputs are moving either to the same, orthogonal or opposite directions relative to each other. This direction dependent summation in MST indicates specific, context dependent selection of input signals. Such a mechanism could be the basis for increased specificity of MST neurons to complex motion patterns.

Introduction

The mammalian visual system is hierarchically organized into a succession of processing stages along the visual pathway. Receptive field size and complexity increase at higher processing stages. A comparison of middle temporal (MT) and medial superior temporal (MST) cortical areas is a clear example for this tendency. Neurons in MT respond selectively to the direction of local visual motion (Rodman and Albright, 1987). MT neurons supply afferents to area MST (Ungerleider and Desimone, 1986), which contains neurons responding selectively to optic flow components, such as expansion, contraction, clockwise or counterclockwise rotation (Sakata et al., 1985, 1986; Saito et al., 1986; Duffy and Wurtz, 1991a,b; Orban et al., 1992; Lagae et al., 1994; Orban et al., 1995; Geesaman and Andersen, 1996; Lappe et al., 1996; Heuer and Britten, 2004) and its linear combinations (Graziano et al., 1994). Because the receptive fields of MST neurons are substantially larger and more complex than that of their inputs (Lagae et al., 1994; Raiguell et al., 1997), MST neurons apparently integrate local motion signals from area MT neurons. However, it is not clear how exactly these complex receptive fields are build up from their simpler inputs.

One explanation for the selectivity of MST neurons for complex motion patterns is a template or mosaic model, in which local motion inputs in MT are lined up according to the preferred complex motion pattern of the MST cells (Tanaka et al., 1989; Duffy and Wurtz, 1991; Perrone and Stone, 1994; Lappe et al., 1996; Beintema and van den Berg, 1998; Royden, 2003;). These selected local motion inputs could be summed in a linear or a nonlinear fashion, depending only on the strength of the input signals, similar to what has been shown in area MT (Britten and Heuer, 1999; Heuer and Britten, 2002) and area MST (Recanzone et al., 1997). In contrast to these models, summation of local motion inputs could also depend on other properties such as the preferred direction of the local motion input signals. It is possible that summation is dependent on specific combinations of local motion signals that are characteristic to complex motion patterns. These interactions would increase the cell's selectivity for complex motion. These properties are suggested because it has been shown for instance that most MST neurons respond to complex motion patterns but not all to the separate local components of those patterns (Duffy and Wurtz, 1991). In this paper we will investigate whether besides linear summation and general non-linearities, interactions between different local motion directions occur in MST.

To test whether MST responses are summed in a direction specific manner we measured the summation properties of MST cells for multiple local stimuli moving in different directions. We presented stimuli moving

simultaneously in four different directions (left, right, up and down) at different locations within the receptive field. A large variety of possible pairs of local motion inputs was constructed this way. The simultaneous stimulation paradigm allowed us to examine the effect of a large number of stimulus combinations, which would be difficult if these combinations were presented individually. In this study, we examined if summation of stimulus pairs moving either in the same, orthogonal or opposite direction would be different from each other. The differences in summation that we report could be the basic mechanism that, besides linear summation, makes MST neurons even more selective for specific complex motion patterns.

Methods

Preparation

This study used three adult female rhesus macaques (*Macaca mulatta*). Before recording, each had been trained to fixate stationary targets in the presence of visual stimuli. Each was implanted with a scleral search coil (Judge et al., 1980) and equipped with a stainless steel head restraint post and recording cylinder located over the occipital cortex. A plastic grid secured inside this cylinder provided a coordinate system of guide tube support holes at 1 mm intervals (Crist et al., 1988). Animal procedures complied with the Institute for Laboratory Animal Research Guide for the Care and Use of Laboratory Animals and were approved by the University of California Davis Animal Care and Use Committee.

On recording days, guide tubes were inserted transdurally through these holes, and Parylene-insulated tungsten microelectrodes were inserted through the guide tubes. Initial mapping penetrations located the superior temporal sulcus (STS) and identified approximate boundaries of the motion-sensitive areas in its depths. MST was identified according to previously published methods (Celebrini and Newsome, 1994). To identify the STS, we used a combination of anatomical and physiological landmarks, including the depth from the brain surface, grey matter/white matter transitions, sulcus crossings and response properties. Within the STS, we located and mapped MT on the posterior bank, using its well-understood and consistent retinotopy and responses for physiological confirmation. MST was encountered after crossing the STS to its anterior bank and was identified by large receptive fields that often included the fovea or extended substantially into the ipsilateral hemifield. In addition, cells on the anterior bank often showed MST-like stimulus selectivities, preferring rapidly moving stimuli and complex optic flow stimuli. All recordings reported here came from penetrations in which the lumen of the STS were crossed and thus most likely from the dorsal subdivision of MST (MSTd). Histological verification

of recording sites has not yet been obtained, as all three monkeys are still being used in related experiments.

Once MST was localized, we would record and isolate activity using standard extracellular methods. Electrode signals were amplified and filtered, and single spikes were converted to digital pulses, whose time of arrival would be recorded with 1 msec resolution using the public domain software package REX (Hays et al., 1982). Search stimuli were chosen to match local multiunit preferences and could be moving bars, dot fields, or Gabor motion impulse stimuli. Once a cell was isolated, its receptive field location was crudely mapped using hand-held, moving bar stimuli, and quantitative testing commenced.

Stimuli.
All stimuli were presented on the face of a cathode ray terminal monitor, subtending 80° horizontally by 60° vertically (1280 x 1024 pixels), operating at a vertical refresh rate of 72 Hz and at a distance of 23 cm. Stimuli were generated by a Pentium personal computer running custom software hosting an ATI Technologies (Thornhill, Ontario, Canada) Mach 64 video card, running in 8 bit mode. Screen luminance was measured as a function of gray scale value using a Tektronix (Wilsonville, OR) photometer, fitted with a cubic polynomial; this was inverted to establish a linearized, gray scale lookup table. Average screen luminance was set to 30 cd/M^2, and maximum achievable contrast was effectively 100% (background luminance was 0.1 cd/M^2).

Stimuli for these experiments were similar to those described by Britten and Heuer (1999) and Heuer and Britten (2002). Stimuli were moving, two-dimensionally oriented "motion impulses," whose spatial luminance function was a Gabor function, or the product of a sine wave and a Gaussian function. These are members of the family that Watson refers to as "generalized Gabors" (Watson and Turano, 1995), which have the property that both the carrier (the sine wave) and the Gaussian contrast envelope are free to move. In our case, carrier and envelope moved together in one of four different directions. The motion directions were always horizontally left or right, or vertically up and down on the screen. The space–time luminance was described by the function:

$$L(x,y,t) = C(t) * \exp\left[-\frac{(x-\mu_x)^2}{\sigma_x^2}\right] * \exp\left[-\frac{(y-\mu_y)^2}{\sigma_y^2}\right] * \sin(\omega x) \quad (1)$$

where (μ_x, μ_y) are the instantaneous location of the center of the impulse, and (σ_x,σ_y) describe its dimensions. The constant ω establishes the spatial frequency of the carrier. The *x* coordinate of the center of the impulse moved linearly in time, and the spatial offset per frame was usually set to one-fourth of the cycle of the carrier. The contrast function *C*(*t*) was a trapezoid spanning seven frames (98 msec) as illustrated in Figure 1 of Britten (1999). The values for these parameters were 1.07 cycles/deg carrier spatial frequency, 18 Hz temporal frequency, σ_x= 0.56°, and σ_y= 1.12. We used these same stimulus settings for all recordings. The diameter of the Gabor functions was 1.5 deg.

Nine of these Gabor motion impulses were positioned along a grid as shown in Fig. 1. We used the same stimulus configuration and dimensions for all cells. The stimulus grid subtended an area of 12.5x12.5 deg, and was positioned on the most active part of the receptive field of the cell. The direction of each individual Gabor motion impulse was chosen randomly out of the four possible motion directions. All nine Gabor motion impulses were moving simultaneously during the trials.

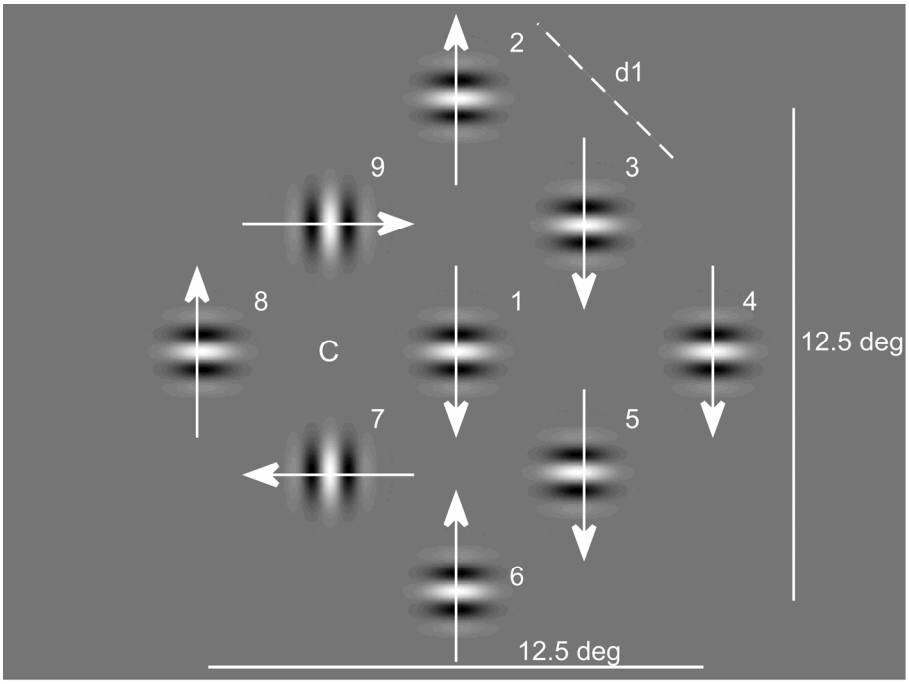

Fig. 1. Illustration of the stimulus field. Individual Gabor motion impulses (as described in the Methods Section) were presented at nine different locations simultaneously according to the configuration indicated in the figure. Each individual Gabor motion impulse could move in four different motion directions, either horizontally left or right or vertically up or down on the screen. The direction of motion for each Gabor motion impulse was chosen randomly and independently. The arrows show a possible combination of motion directions during one motion impulse as indicated by the arrows. The label d_1 indicates the closest distance between two Gabors (4.4 deg). Numbers indicate the reference number of the locations. Each motion impulse lasted 98 msec, which was followed by a 27 ms long blank period when only the gray background was presented. Motion impulses were presented 30 times during one trial, with each time a new randomly-chosen combination of motion directions.

Between each Gabor motion impulse two monitor frames were intervening, which results in a total Gabor motion impulse duration of 125 msec. Gabor motion impulse stimuli were presented sequentially. Single trials consisted of 30 Gabor motion impulse stimuli sequentially with a total duration of 3.8 seconds. The monkey was required to hold fixation during this trial duration and was rewarded for correctly maintaining fixation. There was no inter trial interval, and the monkey was trained to hold fixation over multiple trials. The final motion impulse in trials in which fixation was broken was discarded from subsequent analysis. The trials were run for as long as the cell could be held. In the dataset that we report here, each direction at each location was presented at least 492 times, and on average 2770 times.

Results

We recorded 57 MST neurons in three adult female macaques. The stimulus field consisted of nine Gabor motion impulses arranged along a grid as shown in Fig. 1. The motion directions of the Gabor impulses were randomly chosen and independent from each other. The directions were always either horizontally left or right, or vertically up or down. First, we will document the average response to a single Gabor motion impulse at one location and in one direction; then, we will turn to responses to Gabor pairs.

Response to single Gabor

Before we investigate how responses vary across the receptive field we need to establish an appropriate time window for measuring responses. We calculated the "grand average" PSTH for all cells and all stimulus presentations (Fig. 2). We averaged the responses of each cell for any stimuli and determined the maximal response in the average. We used this maximal response to normalize the cell's response to any stimulus. These normalized responses were then averaged over all cells to produce the histogram. As Fig. 2 shows, response onset starts ~60 ms after stimulus onset, reaches a peak at ~80 ms and decays until ~180 ms, when the response to the following stimulus starts. Notice that the lowest response (~0.62) is still high compared to the dynamic range of the responses (~0.62 - 0.8). This activity does not correspond to spontaneous activity, but is due to the average responses to all stimuli, temporal summation of subsequent stimuli and the different response latencies of individual neurons. Responses to the previous and following stimuli are based on a similar but not completely identical dataset, because the monkey breaks fixation. We chose a time window from 60 to 160 ms to analyze all of the neurons (as indicated in the figure by vertical lines). This way we avoid selecting individual windows for each neuron, which can be unreliable or subjective.

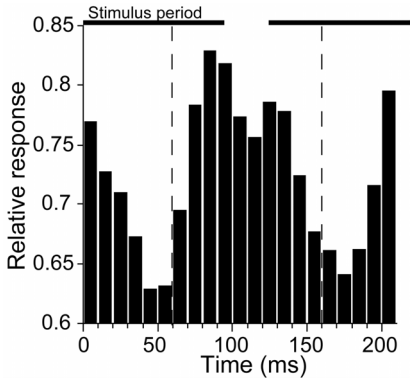

Fig. 2. The time course of responses for the total population. We averaged the responses of each cell for any stimuli and determined the maximal response in the average. We used this maximal response to normalize the cell's response to any stimulus. These normalized responses were than averaged over the whole population to produce the histogram. The vertical dashed lines indicate the boundaries of the temporal window used to calculate average response rates. The bold horizontal line indicates the stimulus period.

Next, we investigated the dependence of responses on location and direction for each cell separately. Figure 3 shows results for an example cell. It illustrates the average response after a specific stimulus occurrence at nine Gabor locations and for four different motion directions. This neuron showed higher activity when a motion direction to the left was presented at nearly all of the nine locations (bottom left panel). For this cell the middle location had the strongest direction selective response. Note that during the experiment, all nine locations were stimulated simultaneously with randomly chosen stimulus directions. Therefore, the calculated average response for each field is a result of the stimulus direction in the corresponding location plus the average response to the randomly-chosen stimulus directions at all other locations. Due to the simultaneous stimulation at multiple locations, these responses are not identical to firing rates evoked by individual Gabors presented alone at different locations. However, these results reveal the spatial dynamic range of the neuron, and its direction tuning at different spatial locations.

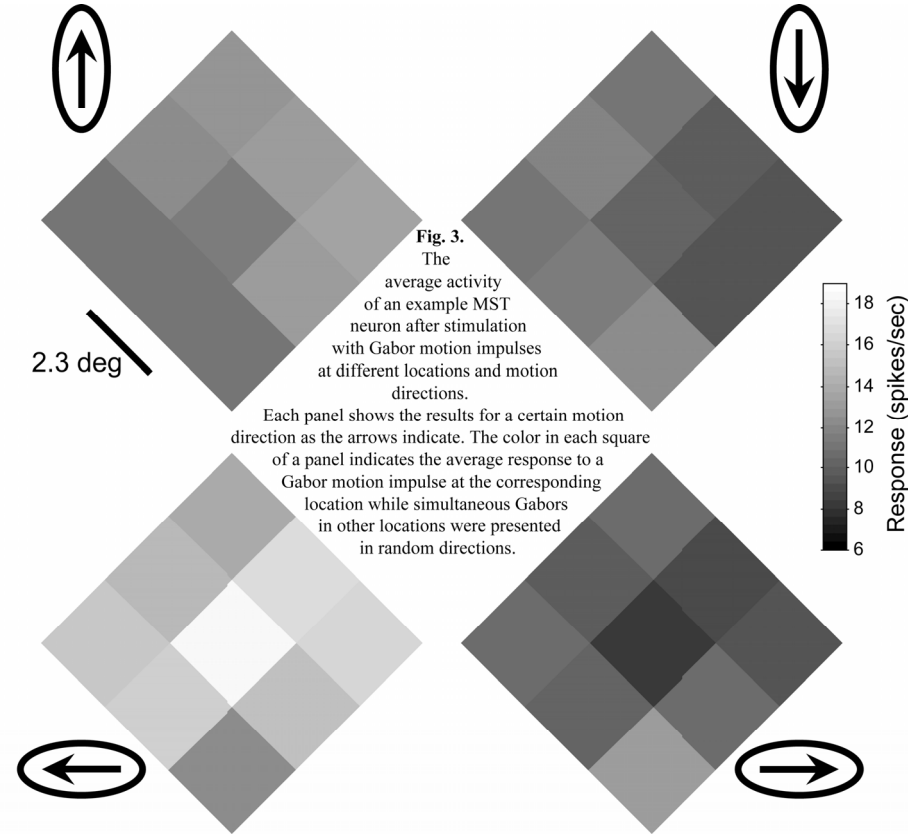

Fig. 3. The average activity of an example MST neuron after stimulation with Gabor motion impulses at different locations and motion directions. Each panel shows the results for a certain motion direction as the arrows indicate. The color in each square of a panel indicates the average response to a Gabor motion impulse at the corresponding location while simultaneous Gabors in other locations were presented in random directions.

It is important to note that the stimulus was not completely balanced, because directions were randomly chosen. The number of stimulus occurrences of one or another direction could be different at a certain location, due to chance variation. However, this unbalance was relatively small compared to the average number of stimulus presentations. To quantify this, we calculated the chance variation (CV) of the stimulus for each cell and stimulus location according to the form:

$$CV = \left(\frac{Count_{\max} - Count_{\min}}{Count_{mean}} \right) * 100 \quad (2)$$

where $Count_{max}$ and $Count_{min}$ indicate the number of presentations of the most often and the least often presented stimulus directions. $Count_{mean}$ indicates the average occurrence of Gabors in any direction. Thus CV expresses the difference between the smallest and largest stimulus occurrence as a percentage of the average stimulus occurrence in any direction. The average CV in the population was 4.3±2.4%, and the most extreme CV for a cell at one Gabor location was 15%.

Response to Gabor pairs

Based on the same data that was used to calculate responses to single Gabors we calculated responses to a combination of two Gabors. Similar to the response to a single Gabor, these average responses are the result of the response to the Gabor pair plus the average response of simultaneously-presented Gabors at other locations to random directions. Both Gabors in the pair could move to any of the four directions and could be presented at any of the nine Gabor locations, resulting in a total number of 1152 possible Gabor pairs. Note that the combination of a location with itself is not included in this subset.

Since Gabors were presented randomly, the number of repetitions for different combinations could be slightly different, and the actual number depended on the duration of the experiment. One specific Gabor pair was presented minimally 102 times and on average 757 times. Similarly to the single Gabor responses, we calculated CV for the Gabor pairs as well, to give an indication about how balanced the stimulus presentation was (equation 2). In this case, $Count_{max}$, $Count_{min}$ and $Count_{mean}$ refer to the occurrence of specific direction combinations rather than directions. The average CV for Gabor pairs was 15±5% and the most extreme CV was 39%. However, even in this case the least number of presentations for a Gabor pair was 185 times.

The main goal of these experiments was to compare responses to Gabor pairs with predicted responses based on the sum of the responses of the same Gabors presented individually. However, there are two reasons why this comparison is not identical to previous summation measurements when predictions to Gabor pairs were based on Gabors presented alone (Britten and Heuer, 1999). First, a substantial part of the response in our measurements is due to Gabors presented at other locations in random directions, resulting in a high baseline activity (see Fig. 2). Second, and more importantly, single responses and pair responses in our paradigm are not independent. Single responses are the result of one particular Gabor combined with all other Gabors, and thus all possible pairs are represented in the single response. Consequently, pair-responses are based on a subset of the single Gabor data.

General linear and nonlinear response summation properties of MT neurons, like a general static non-linearity (saturation) and those reported by Britten and Heuer (1999), re-scale our recorded single and pair responses equally. Therefore, our measurements will not reveal those general linear and nonlinear response properties. However, we are able to investigate nonlinear response summation properties by comparing predicted and measured pair-responses for specific Gabor combinations. As we will show, the relation between predicted and measured responses is different for specific subsets of Gabor combinations, dependent on the relative motion directions and position of the Gabor pairs. These differences indicate specific summation properties in MST that are highly nonlinear, since they depend on the relative directions and positions of the Gabor pairs.

We investigated the differences in response summation for Gabor pairs with same, orthogonal or opposite motion directions. First, we will only discuss the results for the most adjacent Gabor pairs, which were separated by a distance of 4.4 deg (d_1 in Fig. 1). Figure 1 shows examples of these adjacent Gabor pairs for same, orthogonal and opposite directions for locations 3-4, 6-7, and 5-6, respectively. For these most adjacent Gabor pairs, the motion directions are always 45 or 135 deg relative to the line that connects the two positions. The total number of these Gabor pairs in our stimulus is 192.

Figure 4 shows three cells, representative to the range of observations in our data set. In each panel we plotted the observed responses to simultaneous, adjacent Gabor pairs against the predicted response based on the sum of the component single responses. Since the average activity corresponding to the average response to any stimulus was the same for single Gabors and for Gabor pairs, it was necessary to subtract one average

activity from the prediction to bring it into a similar response range as the observed pair responses. The different direction combinations are indicated with different colors. After applying linear regression on the data of the three stimulus conditions separately, it is clear that different direction combinations have different slopes (Fig. 4A and B). In a purely linear system the slopes should be equal to one. The slope differences suggest that the response summation mechanism for different stimulus combinations is not the same.

The cell in Fig. 4C illustrates another characteristic, which we observed only in a small subset of the cells. The slopes for same, orthogonal and opposite direction combinations are very similar, but the linear regression lines are clearly shifted. This indicates that, for this neuron, the measured responses for same direction pairs are generally higher than predicted and for opposite direction pairs generally smaller. The data points are shifted not only for low or high, but in the total range of responses, indicating that the difference in summation mechanism for same and opposite direction is not related to the response level itself. This neuron was one of the clearest examples of this shift; most other neurons only showed slope differences.

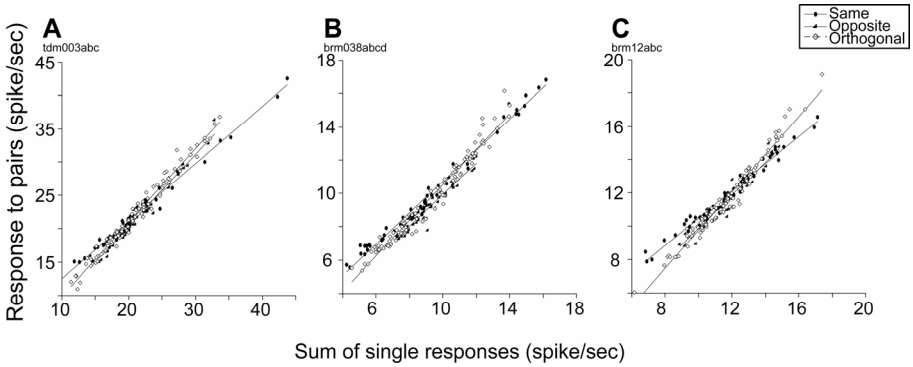

Fig. 4. Summation mechanisms are different for same, orthogonal or opposite direction combinations. Each symbol indicates the measured and predicted response for a pair of adjacent Gabors. Measured responses for Gabor pairs correspond to the average response to certain combinations of two Gabor motion impulses while other stimulus directions in other locations were randomly presented. Predicted responses correspond to the sum of the responses to individual Gabors. The large crosses indicate the average activity to all stimuli. A: Slope for orthogonal direction is the steepest, and same direction is the shallowest. B: Slopes for opposite and orthogonal directions are similar, while the slope for the same direction condition is shallower. C: Opposite directions show lower response than same directions.

To evaluate if two regression lines are significantly different from each other we compared the fit residuals of two linear regressions to the fit residuals of one regression on both groups of points. Evidently, fit residuals

of one linear regression will be larger than residuals for two regressions, because the number of parameters for one regression is less. We used an F-test to evaluate whether the worsening of the fit for one regression is significant, derived under the null hypothesis that the two groups of points are falling on the same line. We performed the test for the combination of any regression lines separately (same/orthogonal, same/opposite and opposite/orthogonal pairs). All of the three example cells in Fig. 4 showed a statistically significant difference between any of two regression lines (F-test, $p<0.05$). For 75% of the cells there was a significant difference between the regression lines of same and orthogonal pairs. For same/opposite and opposite/orthogonal comparison these values were smaller (56% and 38% respectively).

Figure 5 shows the slopes for the three different direction combinations for the whole population. This figure does not only show the slopes for different Gabor pairs, but also how these slopes are related to each other within a cell. The population as a whole shows steeper slopes, higher than 1 for orthogonal (1.07 ± 0.06) pairs and slopes, smaller than 1 for same direction pairs (0.90 ± 0.09). The slopes for opposite directions was on average 0.99 ± 0.11. Slopes for all three directional combinations were statistically significantly different from each other (ANOVA, $p<<0.01$). There was a negative correlation between slopes for same direction pairs and orthogonal direction pairs (Fig. 5A, $r =-0.62$, $p<0.01$) and a weaker, though statistically significant negative correlation between slopes for same/opposite and opposite/orthogonal direction pairs (Fig. 5B, $r =-0.39$ and -0.34 respectively, both p values < 0.05). Filled symbols indicate a statistically significant difference between the two regression lines (F-test, $p<0.05$), according to the statistical method described in the previous paragraph.

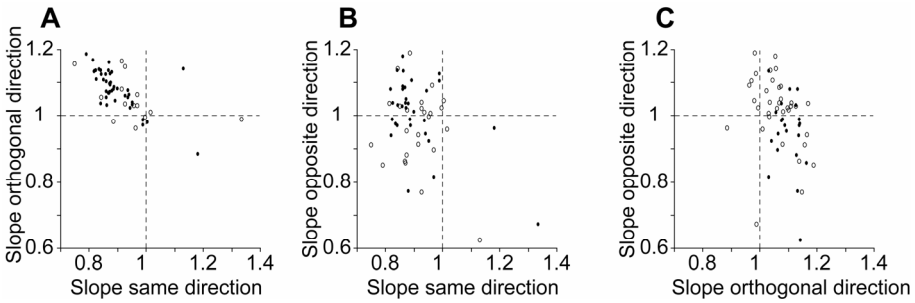

Fig. 5. The slopes of linear regression lines between predicted and measured responses of pairs of Gabors. Each symbol indicates one neuron. A: Slopes for same and opposite direction conditions are negatively correlated. ($r = -0.62$, $p<0.01$) B: Slopes of same and opposite direction conditions are weakly negatively correlated ($r = -0.39$, $p<0.05$). C: Slopes for orthogonal and opposite direction conditions are weakly negatively correlated ($r = -0.34$, $p<0.05$).

Effect of distance

All the preceding analysis was based on pairs of Gabor stimuli, which were the closest to each other. In the following, we investigate the spatial dependence of the spatial summation differences, by describing the slopes of linear fits for the three direction combinations as a function of stimulus distance. The procedure of this analysis was similar to that described above for the most adjacent Gabors. For each stimulus distance, responses to Gabor pairs were plotted against the sum of the component single responses. Linear fits were obtained for same, orthogonal and opposite directional combinations separately.

Figure 6 plots the average slopes of the linear fits for same, orthogonal and opposite Gabor pairs as a function of stimulus distance. The differences between slopes were significantly different for immediately-adjacent Gabor pairs, which we already described in the previous paragraph (ANOVA, $p<0.01$). The slopes were not significantly different for larger stimulus distances, although we still found a significant difference at the largest measured distance of 9.8 deg. Note that because of our stimulus configuration, a different distance also means a change in directions relative to the line that connects the two pairs. Furthermore, the envelope of the Gabor motion impulses was moving, which causes slight differences in distances for the different direction combinations. Therefore, it is not clear from our measurements whether or not the large difference between d_1 and the other distances is a result of the change in distance or in configuration.

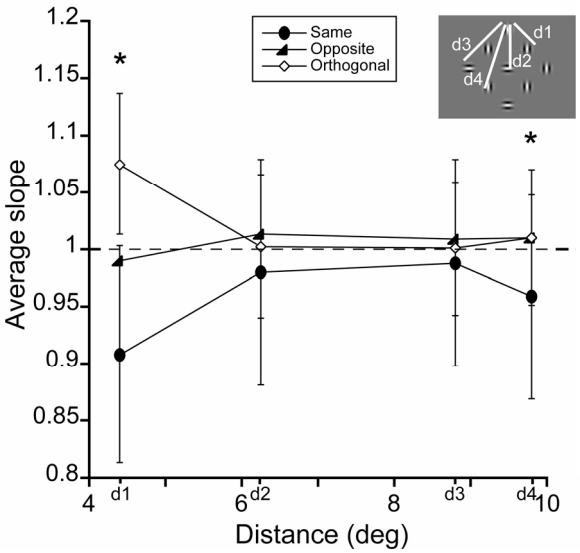

Fig. 6. The slopes of linear regression lines between predicted and measured responses of Gabor pairs as a function of distance. The distances are defined as the inset indicates. The distances for d_1 to d_4 in degrees are 4.4, 6.25, 8.83, and 9.8 deg respectively. The stars above d_1 and d_4 indicate significant differences between the three slopes (ANOVA, $p<0.01$).

Effect of time

We analyzed how the differences in summation mechanism for the three types of directional pairs evolve in time for the most adjacent pairs. We analyzed the slopes of same, opposite and orthogonal Gabor pairs during the time course of the responses. For this analysis, a 60 ms wide window was taken around a series of time points relative to stimulus onset. Figure 7 plots the average slopes as a function at corresponding time points. The average slope for same directions decreases from 1 to about 0.9 in about 100 msec and returns slowly back to 1. The average slopes for orthogonal directions have a similar time course but slopes get higher than 1 up to 1.07. The average slope for opposite directions changes in time. These results indicated different dynamic summation mechanisms for different relative directions.

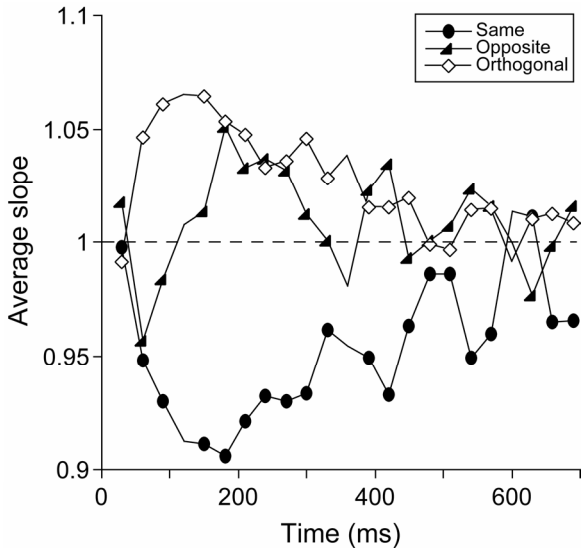

Fig. 7. The temporal development of the different summation properties for pairs of same, orthogonal and opposite direction combinations. The average slope was calculated from responses within a 60 ms wide window centered at different times during the response. Slopes were significantly different from each other at all delays except the first delay (ANOVA, $p<0.01$)

Relationship to tuning in spiral space

If our findings are related to the cell's sensitivity to complex motion patterns, we would expect that specific nonlinearities for directional combinations that we report here are correlated to the tuning of the cells in spiral space (Graziano et al., 1994; Heuer and Britten, 2004). Therefore, we calculated direction indices in spiral space for each neuron.

Since Gabors were presented simultaneously, specific complex motion patterns of four Gabor motion impulses occurred spontaneously. Four Gabor motion impulses can move expanding, contracting or in clockwise or counterclockwise rotation. Those specific combinations occured at least 27 times and on average 217 times at five different locations in the stimulus field. The motion vectors around letter "C" in Fig. 1 illustrate an example of such a complex pattern (clockwise rotation). We calculated the average response after the occurrence of four different complex motion patterns; clockwise rotation, counterclockwise rotation, expanding and contracting patterns. Data for the same complex pattern but at different locations were pooled together. It has been reported that spiral space tuning measured this way correlates strongly with spiral space measurements with four Gabor motion impulses presented alone (not imbedded in simultaneously presented 5 other Gabor motion impulses) or with moving random dots (van Wezel and Britten, 1997).

The Direction Index (DI) for the tuning in spiral space for each cell was calculated based on these four responses by using the method of Baker et al. (1981):

DI = 1 – (non-preferred direction in spiral space / preferred direction in spiral space) (4)

Since we found the largest differences between the regression lines of same and orthogonal direction pairs, we choose the test statistic of the F-test for same/orthogonal regression lines to compare it to the direction index (Fig. 8). Though there was a large variation both in the direction index and the F-value, we found a statistically significant correlation between the cell's sensitivity to specific Gabor combinations and complex motion patterns ($r = 0.39$, $p<0.01$). This indicates that the specific interactions that we describe could be the underlying mechanism for strong selectivity to complex motion in MST neurons.

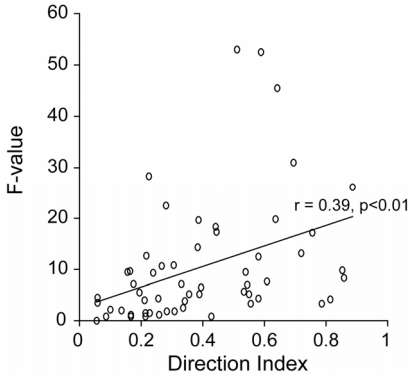

Fig. 8. Differences between same and opposite direction summation are positively correlated to the neuron's sensitivity to complex motion patterns. Each symbol indicates one neuron. The Direction Index corresponds to the cell's tuning in spiral space (see Formula 4. in the Results section). The F-value indicates the difference between same and orthogonal regression lines as indicated in Fig. 4. Larger F-values correspond to larger differences.

Discussion

We investigated spatial summation properties of different stimulus directions within MST receptive fields. Our method does not allow us to test general nonlinearities that operate similarly between a wide range of input signals. However, our analysis can capture specific interactions that might occur, for instance, between certain stimulus locations or by a specific timing of multiple signals. We measured the responses for pairs of Gabors moving in the same, orthogonal or opposite directions. We compared these responses to predicted ones based on the sum of responses to the individual motion directions. We found substantial and consistent differences between summation properties for the three direction combinations. In the following paragraphs we will discuss possible mechanisms causing these differences and their origins.

The slope differences for different Gabor pairs cannot be explained by firing rate dependent general nonlinearities, for instance a static nonlinearity (saturation) at the output of an MST neuron. Other models, such as scaled nonlinear summation models or normalization models (Britten and Heuer, 1999; Recanzone et al., 1997) also fail to describe our data. In area MT and MST, such models have proven to explain summation of two local motion inputs in the same direction, but it can never explain the different summation properties we find when the direction pairs are opposite or orthogonal. To explain our results, such a summation model should include summation properties that are dependent on the angular difference between the two local motion inputs.

Possible sources

Direction specific interactions could arise from local circuits in area MST, at the input of the MST neurons or originate from an earlier processing stage. The spatial extent of the interactions that we find is rather localized (Fig. 6). This indicates that the interactions occur either at the input of the MST cells or at an earlier processing stage with smaller receptive field sizes; at MT, for instance. A similar measurement in MT that targets the summation properties of different stimulus directions could reveal if our results are a specific feature of MST neurons or of direction specific interactions originating from earlier levels.

Slopes for opposite and orthogonal pairs are more similar to each other than are slopes for opposite and same pairs (Fig. 5). This excludes the possibility that the results are only due to orientation differences of the Gabors. When Gabor pairs are presented in the same or opposite directions, the orientations of the Gabors are the same. Therefore, if results were due to interactions between differently tuned cells located, for instance, in V1, we would expect that slopes for the same and opposite direction pairs are more similar than slopes for same and orthogonal pairs, which is not the case. If results were related to cross-orientation inhibition mechanisms (e.g. Blakemore and Tobin, 1972; Kapadia et al., 2000) between the Gabor motion impulses, we would expect that orthogonal Gabor combinations would show the shallower slopes, which it also not the case.

MT cells respond the most to their preferred direction, and in general, the responses are the lowest to the antipreferred direction, which is opposite to the preferred direction (Rodman and Albright, 1987). If our results were related to the tuning properties of MT neurons, we would expect larger differences between opposite and same direction pairs, and smaller differences between opposite and orthogonal pairs, which is exactly the opposite to our findings. The role of center-surround interactions in MT

(Xiao et al., 1995; Born, 2000) can be also excluded, because center-surround interaction is the strongest between opposite directions; therefore, we would expect the largest differences between slopes for the same and opposite direction pairs, and not between the same and orthogonal pairs. Both of these argue against the primary role of MT in the direction-specific interactions.

The most likely locus of direction-specific interactions is between MT and MST. Our results are in accordance with feedback models that assume dynamic feedback loops between MST and MT (Ambastha et al., 2004). In a feedback model, receptive fields are the representations of frequent or useful patterns in their input signals, learned by dynamic feedback loops. These mechanisms could result into the multiplicative and/or recruitement type of nonlinearities that we report, which increase the efficiency of MST neurons to detect complex stimuli. Furthermore, it could explain why certain stimulus combinations, which might be more informative about the complex motion pattern, are summed differently than others. These special mechanisms could be essential for MST to be able to play its important role in complex motion analysis tasks like structure from motion processing (Bradley et al., 1998; Sugihara et al., 2002) and heading detection from optic flow information (Britten and van Wezel, 1998, 2002).

Acknowledgements
We thank Bert van den Berg, Martin Lankheet, André Noest and Henk P. van Wijk for helpful discussions.

References

Ambastha, M., Logan, D., Ballard, D. H., and Duffy, C. J. (2004). Spatial summation data from cortical motion area MST is explained by feedback. Neuroscience 2004 poster.

Baker, J. F., Petersen, S. E., Newsome, W. T., and Allman, J. M. (1981). Visual response properties of neurons in four extrastriate visual areas of the owl monkey (Aotus trivirgatus). J Neurophysiol 45, 397-416.

Beintema, J. A., and van den Berg, A. V. (1998). Heading detection using motion templates and eye velocity gain fields. Vision Res 38, 2155-2179.

Blakemore, C., and Tobin, E. A. (1972). Lateral inhibition between orientation detectors in the cat's visual cortex. Exp Brain Res 15, 439-440.

Born, R. T. (2000). Center-surround interactions in the middle temporal visual area of the owl monkey. J Neurophysiol 84, 2658-2669.

Bradley, D. C., Chang, G. C., and Andersen, R. A. (1998). Encoding of three-dimensional structure-from-motion by primate area MT neurons. Nature 392, 714-717.

Britten, K. H., and Heuer, H. W. (1999). Spatial summation in the receptive fields of MT neurons. J Neurosci 19, 5074-5084.

Britten, K. H., and Van Wezel, R. J. (2002). Area MST and heading perception in macaque monkeys. Cereb Cortex 12, 692-701.

Celebrini, S., and Newsome, W. T. (1994). Microstimulation of extrastriate area MST influences perceptual judgements of motion direction. Invest Ophthal Vis Sci 35, 1828.

Crist, C. F., Yamasaki, D. S. G., Komatsu, H., and Wurtz, R. H. (1988). A grid system and a microsyringe for single cell recording. J Neurosci Meth 26, 117-122.

Duffy, C. J., and Wurtz, R. H. (1991). Sensitivity of MST neurons to optic flow stimuli. I. A continuum of response selectivity of large-field stimuli. J Neurophysiol 65, 1329-1345.

Duffy, C. J., and Wurtz, R. H. (1991). Sensitivity of MST neurons to optic flow stimuli. II. Mechanisms of response revealed by small-field stimuli. J Neurophysiol 65, 1346-1359.

Geesaman, B. J., and Andersen, R. A. (1996). The analysis of complex motion patterns by form/cue invariant MSTd neurons. J Neurosci 16, 4716-4732.

Graziano, M. S. A., Andersen, R. A., and Snowden, R. J. (1994). Tuning of MST neurons to spiral motions. J Neurosci 14, 54-67.

Hays, A. V., Richmond, B. J., and Optican, L. M. (1982). A UNIX-based multiple process system for real-time data acquisition and control. WESCON Conf Proc 2, 1-10.

Heuer, H. W., and Britten, K. H. (2002). Contrast dependence of response normalization in area MT of the rhesus macaque. J Neurophysiol 88, 3398-3408.

Heuer, H. W., and Britten, K. H. (2004). Optic flow signals in extrastriate area MST: comparison of perceptual and neuronal sensitivity. J Neurophysiol 91, 1314-1326.

Judge, S. J., Richmond, B. J., and Chu, F. C. (1980). Implantation of magnetic search coils for measurement of eye position: An improved method. Vision Res 20, 535-538.

Kapadia, M. K., Westheimer, G., and Gilbert, C. D. (2000). Spatial distribution of contextual interactions in primary visual cortex and in visual perception. J Neurophysiol 84, 2048-2062.

Lagae, L., Maes, H., Raiguel, S., Xiao, D. K., and Orban, G. A. (1994). Responses of macaque STS neurons to optic flow components: a comparison of MT and MST. J Neurophysiol 71, 1597-1626.

Lagae, L., Maes, H., Raiguel, S., Xiao, D. K., and Orban, G. A. (1994). Responses of macaque STS neurons to optic flow components: a comparison of MT and MST. J Neurophysiol 71, 1597-1626.

Lappe, M., Bremmer, F., Pekel, M., Thiele, A., and Hoffmann, K. P. (1996). Optic flow processing in monkey STS: a theoretical and experimental approach. J Neurosci 16, 6265-6285.

Orban, G. A., Lagae, L., Verri, A., Raiguel, S., Xiao, D., Maes, H., and Torre, V. (1992). First-order analysis of optical flow in monkey brain. PNAS 89, 2595-2599.

Perrone, J. A., and Stone, L. S. (1994). A model of self-motion estimation within primate extrastriate visual cortex. Vision Res 34, 2917-2938.

Raiguel, S., Van Hulle, M. M., Xiao, D. K., Marcar, V. L., Lagae, L., and Orban, G. A. (1997). Size and shape of receptive fields in the medial superior temporal area (MST) of the macaque. Neuroreport 8, 2803-2808.

Recanzone, G. H., Wurtz, R. H., and Schwarz, U. (1997). Responses of MT and MST neurons to one and two moving objects in the receptive field. J Neurophysiol 78, 2904-2915.

Rodman, H. R., and Albright, T. D. (1987). Coding of visual stimulus velocity in area MT of the macaque. Vision Res 27, 2035-2048.

Saito, H., Yukie, M., Tanaka, K., Hikosaka, K., Fukada, Y., and Iwai, E. (1986). Integration of direction signals of image motion in the superior temporal sulcus of the macaque monkey. J Neurosci 6, 145-157.

Sakata, H., Shibutani, H., Kawano, K., and Harrington, T. L. (1985). Neural mechanisms of space vision in the parietal association cortex of the monkey. Vision Res 25, 453-463.

Sakata, H., Shibutani, H., Ito, Y., and Tsurugai, K. (1986). Parietal cortical neurons responding to a rotary movement of visual stimulus in space. Exp Brain Res 61, 658-663.

Tanaka, K., Fukada, Y., and Saito, H. (1989). Underlying mechanisms of the response specificity of expansion/contraction and rotation cells in the dorsal part of the medial superior temporal area of the
Macaque monkey. J Neurophysiol 62, 642-656.

Ungerleider, L. G., and Desimone, R. (1986). Projections to the superior temporal sulcus from the central and peripheral field representations of V1 and V2. J Comp Neur 248, 147-163.

van Wezel, R. J. A., and Britten, K. H. (1997). Spatial interactions of translational motion impulses in area MST of the macaque monkey. Society for Neuroscience, 23, 15 (abstract).

Watson, A. B., and Turano, K. (1995). The optimal motion stimulus. Vision Research 35, 325-336.

Xiao, D. K., Raiguel, S., Marcar, V., Koenderink, J., and Orban, G. A. (1995). Spatial heterogeneity of inhibitory surrounds in the middle temporal visual area. Proceedings of the National Academy of Sciences of the United States of America 92, 11303-11306.